



UNIVERSITY OF LEEDS

This is a repository copy of *Slag hydration and chloride binding in slag cements exposed to a combined chloride-sulphate solution*.

White Rose Research Online URL for this paper:  
<http://eprints.whiterose.ac.uk/138330/>

Version: Accepted Version

---

**Article:**

Ukpata, JO, Basheer, PAM [orcid.org/0000-0002-0835-8029](https://orcid.org/0000-0002-0835-8029) and Black, L [orcid.org/0000-0001-8531-4989](https://orcid.org/0000-0001-8531-4989) (2019) Slag hydration and chloride binding in slag cements exposed to a combined chloride-sulphate solution. *Construction and Building Materials*, 195. pp. 238-248. ISSN 0950-0618

<https://doi.org/10.1016/j.conbuildmat.2018.11.055>

---

© 2018 Elsevier Ltd. Licensed under the Creative Commons Attribution-NonCommercial-NoDerivatives 4.0 International License (<http://creativecommons.org/licenses/by-nc-nd/4.0/>).

**Reuse**

This article is distributed under the terms of the Creative Commons Attribution-NonCommercial-NoDerivatives (CC BY-NC-ND) licence. This licence only allows you to download this work and share it with others as long as you credit the authors, but you can't change the article in any way or use it commercially. More information and the full terms of the licence here: <https://creativecommons.org/licenses/>

**Takedown**

If you consider content in White Rose Research Online to be in breach of UK law, please notify us by emailing [eprints@whiterose.ac.uk](mailto:eprints@whiterose.ac.uk) including the URL of the record and the reason for the withdrawal request.



[eprints@whiterose.ac.uk](mailto:eprints@whiterose.ac.uk)  
<https://eprints.whiterose.ac.uk/>

1 **Slag hydration and chloride binding in slag cements exposed to a combined**  
2 **chloride-sulphate solution**

3 Joseph O. Ukpata, P. A. M. Basheer and Leon Black

4 School of Civil Engineering, University of Leeds, UK

5

6 **Abstract**

7 The effects of curing temperature (20°C or 38°C), slag composition and slag content  
8 on the hydration and chloride binding characteristics of ground granulated blast-  
9 furnace slag (ggbs) - blended cements have been studied. Two slags ( $\text{CaO}/\text{SiO}_2 =$   
10 1.05 or 0.94) were each blended with CEM I 52.5R at 30% and 70% replacement.  
11 Paste samples of constant 0.5 w/b ratio were hydrated for 56 days, dried and  
12 exposed to either sodium chloride or combined sodium chloride – sodium sulphate  
13 solutions. Sodium sulphate concentration was 3g/L, while chloride concentrations  
14 varied from 0.1 to 3.0M. Post-exposure reaction products were characterised by  
15 XRD and thermal analysis. Chloride binding was followed via Friedel's salt formation,  
16 with thermal analysis showing a decrease in Friedel's salt formation in the presence  
17 of sulphate ions. Increasing slag content changed the nature of the chloride binding  
18 mechanism significantly. Hydration of slag studied by SEM-BSE image analysis  
19 showed that the higher basicity slag was more reactive, with the degree of slag  
20 hydration increasing with temperature. An increase in the slag load reduced the  
21 degree of slag hydration. Apart from the increase in slag load, the other changes in  
22 hydration corresponded well with the chloride binding characteristics of the blends.

23 **Keywords:** chloride, chloride binding, sulphate, slag, cement.

24 **1. Introduction**

25 Corrosion of steel reinforcement bars is a major problem affecting the durability of  
26 reinforced concrete structures located in marine environments. Structures may often

27 suffer deterioration arising from the corrosion of reinforcing steel bars due to chloride  
28 attack. This undermines the structural integrity of the steel bars, with adverse  
29 implications for design service lives. Studies have reported that chloride ions are  
30 either bound to the binder paste component of the concrete matrix, or freely held in  
31 pore solutions within the matrix. It is the free chloride ions in the pore solutions that  
32 are responsible for causing the corrosion of embedded steel bars

33 Bound chloride ions do not contribute to corrosion of embedded steel in concrete  
34 structures [1-3]. Therefore, durability is ensured by reducing porosity and increasing  
35 the chloride binding capacity of concrete. Supplementary cementitious materials  
36 (SCMs), such as slag, are known to have good chloride binding capacity [4, 5]. This  
37 would ensure that any residual chloride ions penetrating the concrete matrix are fully  
38 or partially bound by the blended cement component of the concrete. The combined  
39 strategy would enhance reduction in the concentration of free chlorides such that any  
40 remaining chloride ions in the concrete matrix do not reach the chloride threshold  
41 necessary to initiate steel corrosion.

42 Many studies have indicated that there is a critical concentration of chloride ions for  
43 corrosion initiation in embedded steel to occur [3, 6-8], and the aim of any durability  
44 design against chloride attack must be to keep free chloride concentrations in the  
45 concrete matrix below critical levels. The threshold concentration has been found to  
46 increase in slag-blended cement systems [7] and the incorporation of ggbs (slag)  
47 with high alumina contents in cements is well-known to increase chloride binding  
48 capacity of Portland cements [1, 4, 5, 9, 10].

49 Chloride binding is achieved through both physical and chemical processes. The  
50 physical process is where chloride ions are adsorbed to the surfaces of C-S-H or

51 other phases of hydrated cement, while the chemical process involves reaction of  
52 chlorides with the  $C_3A$ ,  $C_4AF$ , or their hydrates - monosulphates to form Friedel's salt  
53 (FS) and/or Kuzel's salt (KS) [10-15]. However, where NaCl is the exposure solution,  
54 chloride binding in Portland cement is mainly attributed to the formation of FS [16].

55 The binding of chlorides can be affected by several factors [1, 17, 18]. The effects of  
56 external factors such as interaction with other anions, as present in marine  
57 environments, need to be investigated. For example, the presence of external  
58 sulphate ions are known to reduce chloride binding or destabilise already bound  
59 chlorides [1, 19-23]. Meanwhile, an increase in exposure temperature from 20°C to  
60 38°C has been found to increase chloride binding [4, 24]. However, Z ibara [25] found  
61 that the effect of temperature on chloride binding depended on the chloride  
62 concentration of the exposure solution, with increasing temperature decreasing  
63 chloride binding at low concentration (e.g. 0.1M), yet increasing chloride binding at  
64 higher chloride concentration (e.g. 3.0M). Yet, Dousti and Shekarchi [26], in their  
65 study covering a range of temperatures from -4°C to 70°C found that chlori de binding  
66 in plain and blended cements decreased significantly at temperatures beyond 22°C.  
67 This, and other similar works, suggests that more work remains to be done to clarify  
68 the contradictions concerning the effects of temperature on chloride binding of  
69 cementitious materials. Furthermore, studies have found that differences in  
70 associated cations (i.e. Na, Mg, Ca) have significant effects on chloride binding  
71 capacity of cementitious materials [1, 16, 19]. De Weerd et al [27] associated these  
72 effects with changes in pH of the exposure solution and the chloride binding capacity  
73 of the C-S-H phase of hydrated cements.

74 The present study investigates simultaneously the effects of some key factors such  
75 as temperature, presence of external sulphate, slag composition, slag content, and

76 concentrations of the attacking free chlorides, on hydration and chloride binding  
77 characteristics of slag-blended cements, to build on earlier related studies [4, 24].  
78 NaCl, being the most abundant in marine sea water environments [14], is used in  
79 this study as the source of attacking chloride.

## 80 **2. Experimental details**

### 81 2.1 Materials and exposure solutions

82 Two slags similar to those used elsewhere [4, 24, 28-30] were used in this study,  
83 alongside CEM I 52.5 R. The slags have similar physical properties (Table 1 & Fig.  
84 1) but different chemical compositions (Table 2) and both comply with relevant  
85 standards [31, 32]. They have been designated as slags 1 and 2, with slag 1 being  
86 more basic and having a higher alumina ( $Al_2O_3$ ) content, of 12.23% compared with  
87 7.77% for slag 2 (Table 2). As noted previously, alumina is a driver for chloride  
88 binding with higher alumina content favouring improvement in chloride binding  
89 capacity of cement [4, 10]. Blending of slag with CEM I was carried out using a roller  
90 ball mill incorporating plastic charges. Either 30% or 70% of CEM I was replaced  
91 with each of the slags to produce 4 different test binders, shown in Table 3.  
92 Exposure solutions were prepared using standard laboratory reagent grade sodium  
93 chloride and sodium sulphate, which were diluted in deionised water to specified  
94 concentrations in the test method.

95

96 Table 1: Physical properties of cementitious materials

Property	Unit	CEM I 52.5R	Slag 1 (S1)	Slag 2 (S2)
Blaine	cm <sup>2</sup> /g	7357	5995	5540
Density	g/cm <sup>3</sup>	3.16	2.93	2.91
D10	µm	2.94	2.27	2.87
D50	µm	9.43	11.56	12.91

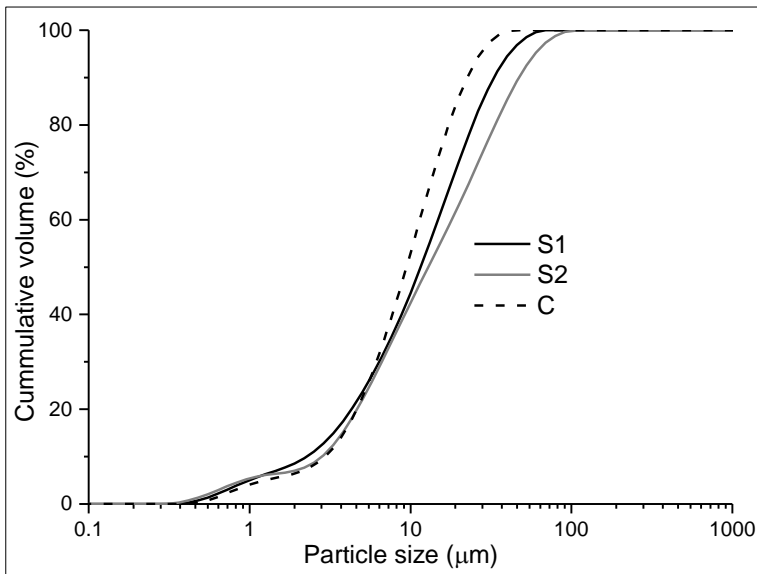
97

98

99 Table 2: Chemical compositions of cementitious materials

Property	Unit	CEM I 52.5R	Slag 1 (S1)	Slag 2 (S2)
SiO <sub>2</sub>	%	20.50	36.58	40.14
Al <sub>2</sub> O <sub>3</sub>	%	5.43	12.23	7.77
TiO <sub>2</sub>	%	0.29	0.83	0.30
MnO	%	0.05	0.64	0.64
Fe <sub>2</sub> O <sub>3</sub>	%	2.51	0.48	0.78
CaO	%	63.43	38.24	37.90
MgO	%	1.51	8.55	9.51
K <sub>2</sub> O	%	0.79	0.65	0.55
Na <sub>2</sub> O	%	0.17	0.27	0.36
SO <sub>3</sub>	%	3.43	1.00	1.47
P <sub>2</sub> O <sub>5</sub>	%	0.14	0.06	0.02
LOI 950°C	%	1.37	1.66	0.40
Total	%	99.62	99.88	99.43
Glass content	%	na	99.3	97.1
CaO/SiO <sub>2</sub>		Na	1.05	0.94
(CaO + MgO) / SiO <sub>2</sub>		Na	1.28	1.18
<b>Phase compositions:</b>				
C <sub>3</sub> S	%	58.5	Na	na
C <sub>2</sub> S	%	14.4	Na	na
C <sub>3</sub> A	%	10.7	Na	na
C <sub>4</sub> AF	%	7.0	Na	na
Calcite	%	0.8	Na	na

100



101

102 Fig. 1. Particle size distribution of cementitious materials

103

104 Table 3: Test binders configuration

Binder	Binder component (wt. %)			w/b
	CEM I (PC)	Slag 1 (S1)	Slag 2 (S2)	
30S1	70	30	-	0.5
30S2	70	-	30	0.5
70S1	30	70	-	0.5
70S2	30	-	70	0.5

105

106 2.2 Test methods

107 2.2.1 Chloride binding

108 The chloride binding test method was similar to the equilibrium method developed by  
 109 Tang and Nilsson [33] which has been used regularly [4, 10, 34]. Two sets of paste  
 110 samples cast in 30ml plastic vials at 0.5 w/b ratio were sealed, rotated for 24 hours  
 111 at 20rpm to prevent bleeding, and then stored in vacuum-sealed plastic bags to cure  
 112 in water baths set at 20°C or 38°C for 56 days, followed by crushing, drying and  
 113 exposure to test solutions. The paste samples were crushed to particle sizes ranging  
 114 from 0.075 – 2.0mm. Drying for the first 3 days was done in a desiccator containing  
 115 silica gel and soda lime under low vacuum (0.75bar) to remove excess water,  
 116 followed by further 14 days drying at 11% relative humidity in a CO<sub>2</sub>-free desiccator  
 117 containing soda lime and saturated lithium chloride solution. Drying to 11% RH was  
 118 found to be appropriate for studying the stoichiometry of C-S-H, providing a good  
 119 basis for any estimate of absorbed water [33, 35]. Both drying regimes were  
 120 implemented under laboratory-ambient temperature of 23±1°C, to preserve the paste  
 121 microstructure. The hydrated paste samples were soaked in parallel solutions of  
 122 pure NaCl (0.1 – 3.0M), and combined NaCl (varying concentration: 0.1, 0.3, 0.5,  
 123 0.7, 1.0, 2.0, & 3.0M) plus Na<sub>2</sub>SO<sub>4</sub> (fixed: 0.021M or 3g/L typical of the  
 124 concentrations found in seawater and in line with a previous study [36, 37]) in 125ml  
 125 plastic bottles at liquid to solid ratio of 4. The mixtures were saturated with Ca(OH)<sub>2</sub>  
 126 to prevent leaching, sealed with the bottles' lids and stored in the laboratory, at

127 temperatures of 20°C and 38°C. The 38°C oven-stored samples were further sealed  
128 using parafilm to prevent evaporation. The soaked samples were stored for 42 days  
129 to reach equilibrium concentration between the bound and free chloride ions [4]. This  
130 was checked by weekly measurements of free chloride concentrations in the 3.0M  
131 solutions, assuming these would take longer to attain equilibrium than samples of  
132 lower chloride concentrations [10]. Chloride ion concentrations were measured by  
133 ion chromatography, using Metrohm 850 professional IC / 896 detector equipped  
134 with an automatic sample processor. Bound chloride was calculated from Equation  
135 1.

136

$$C_b = \frac{35.45 V (C_i - C_f)}{W_d} \quad (1)$$

137 Where:

138  $C_b$  = bound chlorides (mg/g of sample);

139  $C_i$  = initial chloride concentration (mol/l);

140  $C_f$  = free chloride concentration at equilibrium (mol/l);

141  $V$  = volume of external chloride solution (ml); and

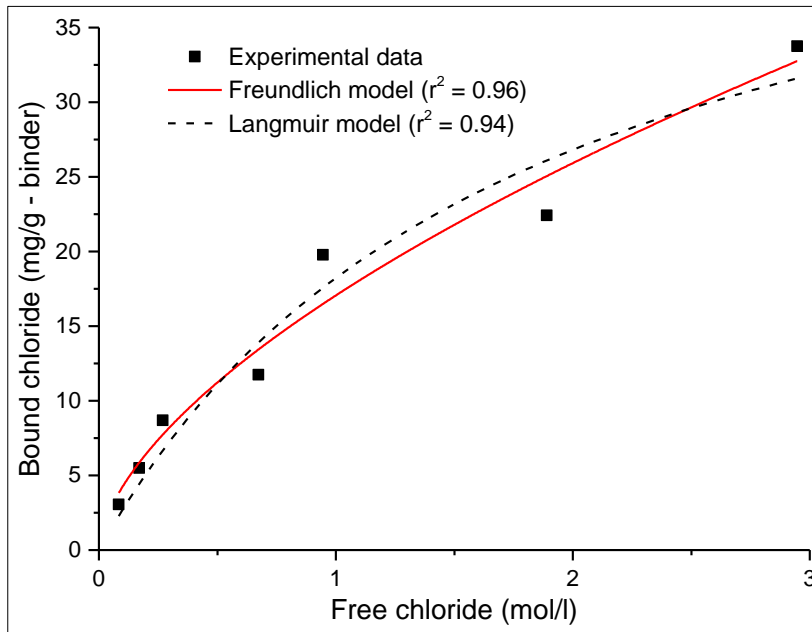
142  $W_d$  = mass of dry sample (g).

143

144 At equilibrium, bound chlorides (mg/g of binder) were plotted against free chlorides  
145 (mol/l) to obtain the chloride binding relationships (isotherms) for the various test  
146 binders (Fig.2). The 2 well-known chloride binding models, Langmuir (Equation 2)

147 and Freundlich (Equation 3) isotherms were used to fit the experimental data to  
 148 obtain 'best fit' chloride binding coefficients ( $\alpha$  and  $\beta$ ) for the test binders (Table 4).

149



150

151 Fig. 2. Best fit chloride binding isotherms.

152 
$$C_b = \frac{\alpha \cdot C_f}{(1 + \beta \cdot C_f)} \quad (2)$$

153 
$$C_b = \alpha \cdot C_f^\beta \quad (3)$$

154

155 2.2.2 X-ray diffraction (XRD)

156 Crystalline hydration products were followed using a Bruker D2 phaser diffractometer  
 157 with a Cu K $\alpha$  source, operating at 30 KV and 10 mA. Scanning was performed on  
 158 back-loaded, powdered samples from 5° to 70°: 2 $\theta$ , at 0.034° increment with a scan  
 159 time of 2 s and sample rotation of 15/min. Phases were identified using BRUKER  
 160 XRD DIFFRAC.SUITE V3.0 software.

161

162 2.2.3 Thermal analysis

163 Thermogravimetric analysis (TGA) was performed on powdered samples using a  
164 Stanton Redcroft 780 series thermal analyser. The samples were heated under  
165 nitrogen (at a flow rate of 50 ml/min) up to 1000°C, at a heating rate of 20°C/min.  
166 The initial sample masses were kept between 15 and 17 mg. The weight losses due  
167 to phase changes were used to identify and quantify hydration products such as  
168 portlandite (CH) and Friedel's salt (FS).

169

#### 170 2.2.4 Degree of hydration by SEM/EDX image analysis (IA)

171 The degrees of clinker and slag hydration were investigated using scanning electron  
172 microscopy/ energy dispersive x-ray spectroscopy (SEM/EDX), image analysis of  
173 backscattered electron (BSE) images in conjunction with EDX magnesium maps.  
174 These were acquired using Zeiss EVO MA 15 SEM equipped with Oxford  
175 Instruments X-max SDD EDX detector. 30 BSE images and corresponding EDX  
176 maps were obtained per sample, at 800x magnification and working distances  
177 between 8 and 9mm, using an accelerating voltage of 20KeV. Image analysis was  
178 carried out using ImageJ software in line with previous studies [38, 39].

179

### 180 **3. Results and discussion**

#### 181 3.1 Chloride binding

182 The relationships between bound and free chlorides were fitted by both Freundlich  
183 and Langmuir isotherms to determine chloride binding coefficients (Table 4). The  
184 Freundlich model generally showed better fit of the experimental data consistent with  
185 other findings [1, 4, 10, 33, 34]. Langmuir isotherms normally assume a monolayer,

186 while Freundlich isotherms assume more than a single layer, and are hence more  
 187 consistent with the binding process investigated here. The chloride binding of  
 188 samples exposed to pure chloride solutions fitted the 2 isotherms better with the  
 189 adjusted  $r^2$  values mostly greater than 0.90. It is presumed that the changes in phase  
 190 assemblage due to the interactions between the cement paste and the sulphate ions  
 191 in solution (see below) brings about changes in chloride binding reflected in the  
 192 diminished quality of fit for the two isotherms described above.

193

194 Table 4. Chloride binding coefficients

Binder	Exposure solution	Temp. (°C)	Freundlich model			Langmuir model		
			$\alpha$	B	Adj. $r^2$	$\alpha$	$\beta$	Adj. $r^2$
30S1	NaCl + Na <sub>2</sub> SO <sub>4</sub>	20	14.68	0.33	0.74	53.35	2.33	0.81
30S1	NaCl	20	18.14	0.51	0.98	35.68	0.82	0.90
30S1	NaCl + Na <sub>2</sub> SO <sub>4</sub>	38	14.95	0.42	0.88	36.98	1.29	0.86
30S1	NaCl	38	20.17	0.57	0.97	34.29	0.60	0.92
70S1	NaCl + Na <sub>2</sub> SO <sub>4</sub>	20	25.05	0.41	0.62	91.79	2.24	0.66
70S1	NaCl	20	21.87	0.55	0.94	40.38	0.70	0.87
70S1	NaCl + Na <sub>2</sub> SO <sub>4</sub>	38	24.59	0.68	0.88	34.45	0.35	0.85
70S1	NaCl	38	25.52	0.65	0.96	40.60	0.46	0.96
30S2	NaCl + Na <sub>2</sub> SO <sub>4</sub>	20	12.67	0.41	0.66	33.05	1.40	0.68
30S2	NaCl	20	18.35	0.57	0.97	30.32	0.56	0.91
30S2	NaCl + Na <sub>2</sub> SO <sub>4</sub>	38	12.69	0.48	0.73	27.70	1.02	0.77
30S2	NaCl	38	18.19	0.61	0.98	28.11	0.46	0.94
70S2	NaCl + Na <sub>2</sub> SO <sub>4</sub>	20	17.06	0.60	0.96	28.44	0.56	0.94
70S2	NaCl	20	19.94	0.76	0.99	25.87	0.24	0.99
70S2	NaCl + Na <sub>2</sub> SO <sub>4</sub>	38	19.65	0.70	0.93	25.80	0.28	0.91
70S2	NaCl	38	22.33	0.74	0.99	30.51	0.28	0.99

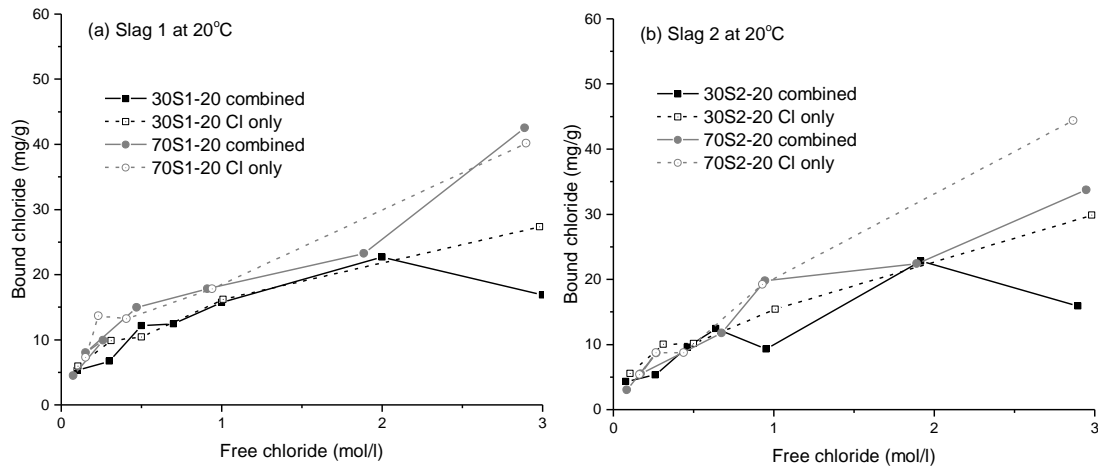
195

### 196 3.1.1 Influence of slag load, slag composition and external sulphate

197 Generally, chloride binding in combined solutions was lower than in pure chlorides in  
 198 line with the literature [1, 40], although the presence of sulphates did lead to less  
 199 clear cut trends, reflective of the lower  $r^2$  values. A similar observation was reported

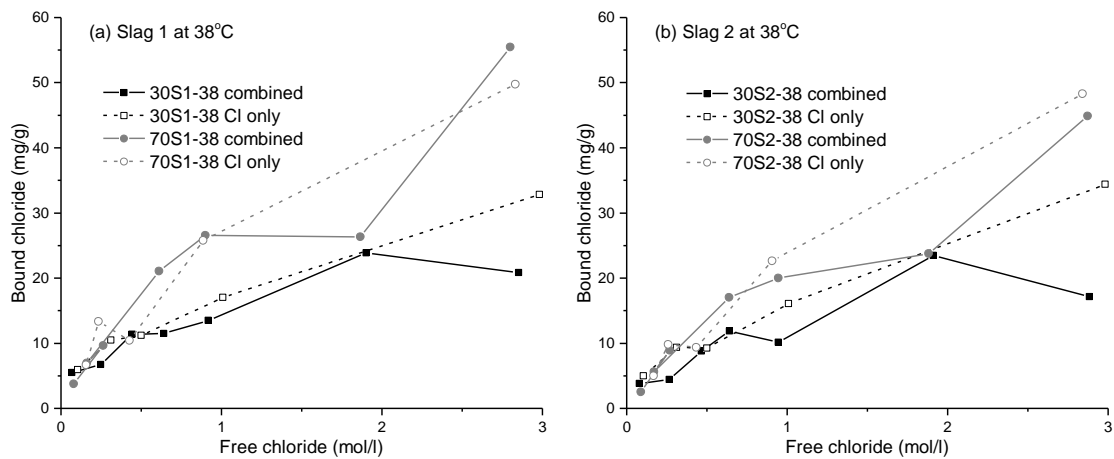
200 by Maes [40], concerning chloride ingress from a combined chloride-sulphate  
201 solution. However, most previous studies used much higher concentrations of  
202 sulphate [21, 22, 40-42], although chloride binding was still reduced at the  
203 concentrations used here, which are comparable to Zibara [25].

204 The influences of slag load and slag composition on chloride binding are presented  
205 in Figures 3 and 4 for exposure at 20°C and 38°C respectively ly. Increasing the slag  
206 content in the blends from 30 to 70% generally increased chloride binding for both  
207 slags and temperatures, consistent with the literature [43]. Improved resistance to  
208 chloride penetration due to increasing slag replacement has been attributed to  
209 increased chloride binding resulting from increased C-A-S-H formation, in addition to  
210 pore refinement of the concrete [5, 14, 15]. Figures 3 and 4 also show the effects of  
211 an external sulphate source. At both temperatures, the presence of sulphate caused  
212 a slight decrease in the chloride binding of all the samples, when the free chloride  
213 concentration was less than 1.0 mol/l. A possible reason for this is the preferential  
214 reaction of sulphate with C<sub>3</sub>A and C<sub>4</sub>AF or their hydrates to form ettringite, which  
215 inhibits the formation of Friedel's salt (3CaO.Al<sub>2</sub>O<sub>3</sub>.CaCl<sub>2</sub>.10H<sub>2</sub>O) or Kuzel's salt  
216 (3CaO.Al<sub>2</sub>O<sub>3</sub>.0.5CaCl<sub>2</sub>.0.5CaSO<sub>4</sub>.11H<sub>2</sub>O) responsible for the chemically bound  
217 chlorides [41, 44]. The decrease in chloride binding however, appears less severe at  
218 high slag load, again consistent with the literature [5]. Increasing slag content is  
219 known to increase chloride resistance of slag-blended systems due to increased  
220 aluminate content and the increased presence of C-A-S-H brought about by the slag  
221 hydration [45, 46].



222

223 Fig. 3. Chloride binding isotherms: influence of external sulphate at 20°C.



224

225 Fig. 4. Chloride binding isotherms: influence of external sulphate at 38°C.

226

227 3.1.2 Influence of slag composition and temperature

228 Higher temperatures increased the bound chloride content. This may be explained

229 by the higher degree of hydration when curing slag cements at higher temperatures

230 (Table 5). The chloride binding isotherms for the investigated slag pastes are shown

231 in Figures 5 and 6 for 30% and 70% slag blends respectively. These figures highlight

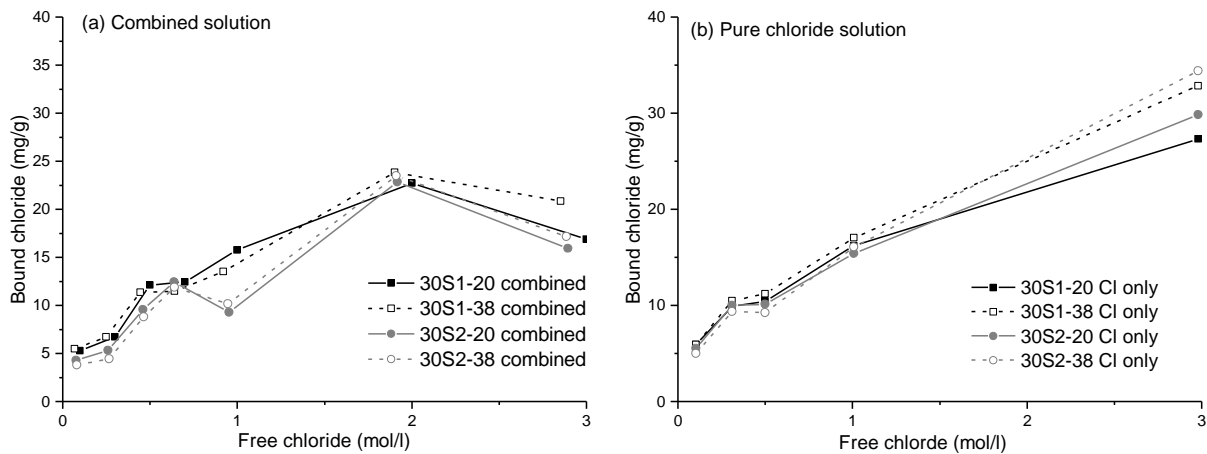
232 the effects of slag composition and temperature on chloride binding. The more basic,

233 alumina-rich slag 1 blends generally bound more chlorides than the equivalent slag 2

234 blends at both exposure temperatures, although the opposite was observed in a

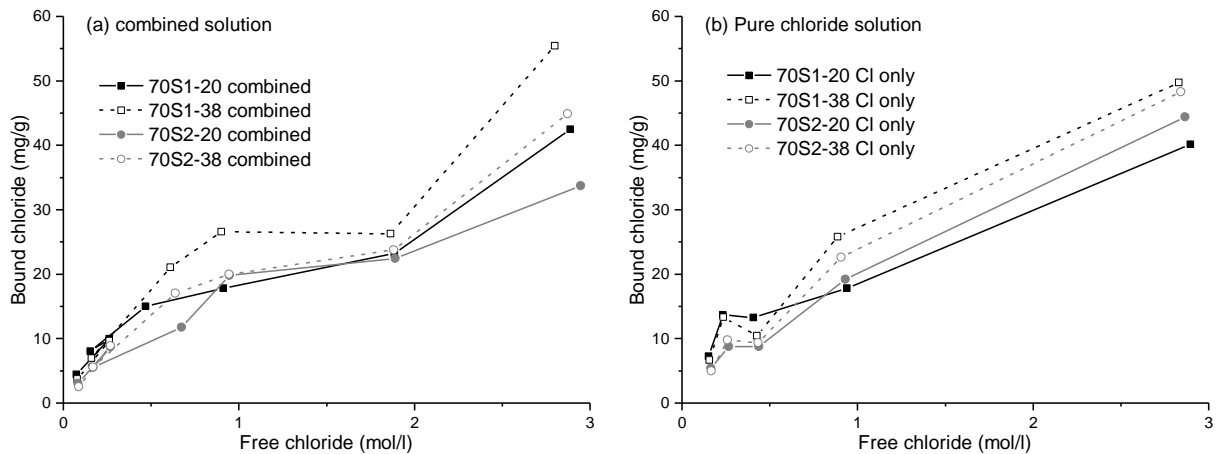
235 single instance (exposure to pure chloride solution at 20°C) (Figs. 5b & 6b) at

236 concentrations greater than about 1.0M. The reason for this is not clear. However,  
 237 increasing alumina contents of binders have been reported to have a positive impact  
 238 on chloride binding [4, 10, 47]. Temperature had a greater influence than slag  
 239 composition for both slag loadings, but particularly at 70% slag replacement. This  
 240 reflects the positive role of slags in chloride binding. Typically, increased temperature  
 241 led to improved chloride binding capacity in the paste blends, especially at higher  
 242 chloride concentrations [4, 25]. However, this effect was only slight at low free  
 243 chloride concentrations (<1.0 mol/l). This is in agreement with previous findings [25].  
 244 The bound chloride contents were generally higher than those reported in the  
 245 literature for plain Portland cements, indicating an increased chloride binding  
 246 capacity of slag-blended cements [1, 10].



247  
 248 Fig. 5. Chloride binding isotherms for 30% slag-blends: influence of temperature

249



250

251 Fig. 6. Chloride binding isotherms for 70% slag-blends: influence of temperature

252

### 253 3.2 X-ray diffraction (XRD) analysis

254 Figures. 7 and 8 show XRD patterns obtained from samples following chloride

255 binding determination at 0.5M and 3.0M free chloride concentrations. The changes in

256 crystalline phase composition are consistent with the hydration and chloride binding

257 characteristics of the slag-blended pastes. All of the samples revealed the formation

258 of Friedel's salt (FS). Hydrated 30% slag blends exposed in the 0.5M solution

259 showed reflections due to ettringite, portlandite and FS as the main crystalline

260 phases, at  $9.1^\circ$ ,  $18.1^\circ$  and  $11.2^\circ$   $2\theta$  respectively. The intensities of their reflections

261 reduced with 70% slag content of the blends, while Kuzel's salt (KS) was formed,

262 with a reflection at  $10.5^\circ$   $2\theta$ , along with FS. These correspond with the weighted

263 degrees of hydration of the blends, which decreased with increased slag contents.

264 However, as the concentration of chloride in the solution was increased to 3.0M,

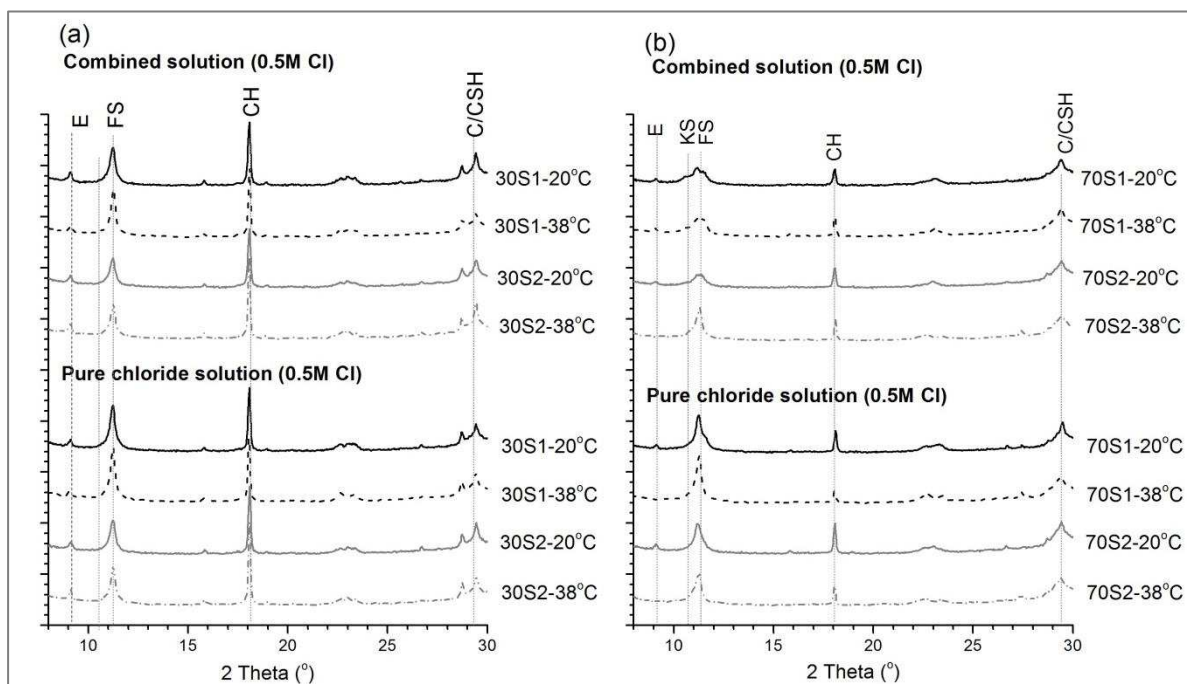
265 ettringite was almost absent, while FS reflection increased significantly. The

266 relationships between the 2 blends were similar with samples exposed in 0.5M

267 chloride solution.

268 The 30% slag blends showed increased levels of Friedel's salt both when the  
 269 samples had been cured at 38°C, and when using the alumina-rich more basic slag  
 270 1. These observations are consistent with previous findings, namely that for systems  
 271 dominated by cement clinker, then exposed to NaCl solutions, chloride binding is  
 272 mainly defined by the formation of Friedel's salt [16, 17, 26].

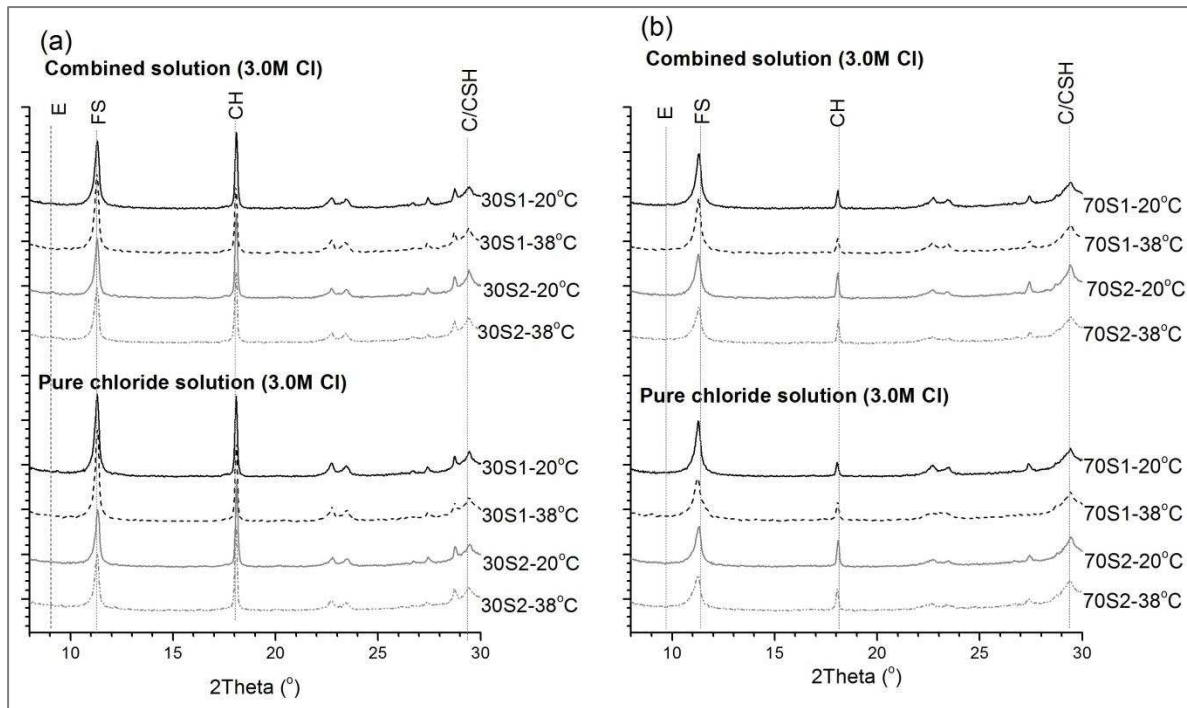
273



274

275 Fig. 7. XRD patterns of pastes exposed to NaCl and combine NaCl plus Na<sub>2</sub>SO<sub>4</sub>  
 276 solutions (C<sub>f</sub> = 0.5M). C: calcite; CH: portlandite; CSH: calcium-silicate-hydrate; E:  
 277 ettringite; FS: Friedel's salt; KS: Kuzel's salt.

278



279

280 Fig. 8. XRD patterns of pastes exposed to NaCl and combine NaCl plus Na<sub>2</sub>SO<sub>4</sub>  
 281 solutions (C<sub>f</sub> = 3.0M). C: calcite; CH: portlandite; CSH: calcium-silicate-hydrate; E:  
 282 ettringite; FS: Friedel's salt.

283

284 Less intense Friedel's salt reflections were found however in the samples exposed to  
 285 a combined chloride-sulphate solution, confirming the negative impact of sulphate on  
 286 chloride binding. At high slag load, it is possible that the dominant C-A-S-H phase  
 287 formation would require a source of calcium which then destabilises FS formation.  
 288 This dominant pozzolanic reaction is confirmed by CH consumption, evidenced by  
 289 the weaker reflections for the 70% blends (Figs 7b & 8b).

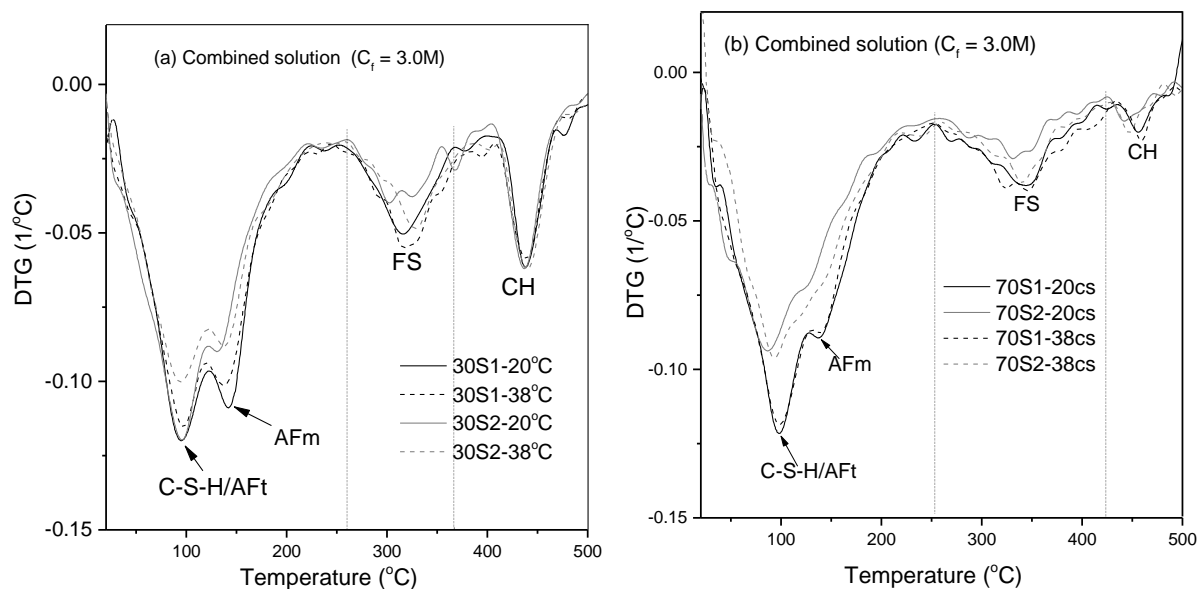
290 For samples exposed to combined chloride – sulphate solutions, higher chloride  
 291 concentrations lead to displacement of sulphate as shown in Fig.8. The clear  
 292 ettringite peaks at 0.5M Cl (Fig.7) were absent at 3.0M Cl (Fig.8). Also, Kuzel's salt  
 293 was observed via the reflection at about 10.5° 2θ [48], following exposure to the  
 294 0.5M chloride - sulphate solution at 20°C. This is in line with previous research,  
 295 where it was reported that chloride can displace sulphate from monosulphate to form

296 Kuzel's salt at lower chloride concentration, while FS is formed at higher  
297 concentration [49].

298

### 299 3.3 Thermal analysis

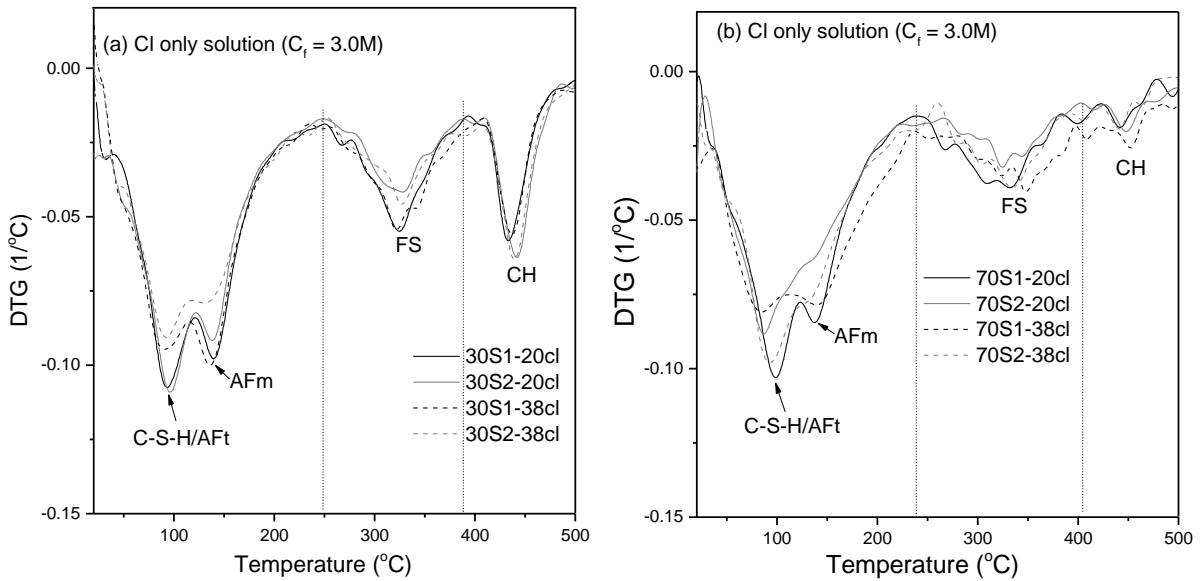
300 Thermogravimetric analysis (TGA) was conducted to confirm and quantify the  
301 phases formed. Figs. 9 and 10 show DTG plots, revealing peaks consistent with  
302 those discussed for XRD. For pastes in combined solutions (Fig. 9), Friedel's salt  
303 decomposed from about 260°C to 370°C for the 30% blends, and a bout 260°C to  
304 430°C for the 70% blends. These range of temperatures are consistent with the  
305 literature for pure FS [50, 51] and FS in plain and composite cements [11, 16, 21].  
306 According to previous studies [11, 16, 52], FS formed in the paste may be identified  
307 from the second of three main DTG peaks, which occurs approximately between  
308 250°C and 420°C, depending on binder type as shown in Figs. 9 and 10. The other  
309 two with mass losses from 100-200°C and 650-750°C are only clearly resolved in  
310 pure FS phase as in [49].



311

312 Fig. 9. DTG plots showing Friedel's salt peaks for pastes exposed to combined NaCl  
313 - Na<sub>2</sub>SO<sub>4</sub> solutions: (a) 30% slag blends, (b) 70% slag blends.

314



315

316 Fig. 10. DTG plots showing Friedel's salt peaks for pastes exposed to pure NaCl  
317 solutions: (a) 30% slag blends, (b) 70% slag blends.

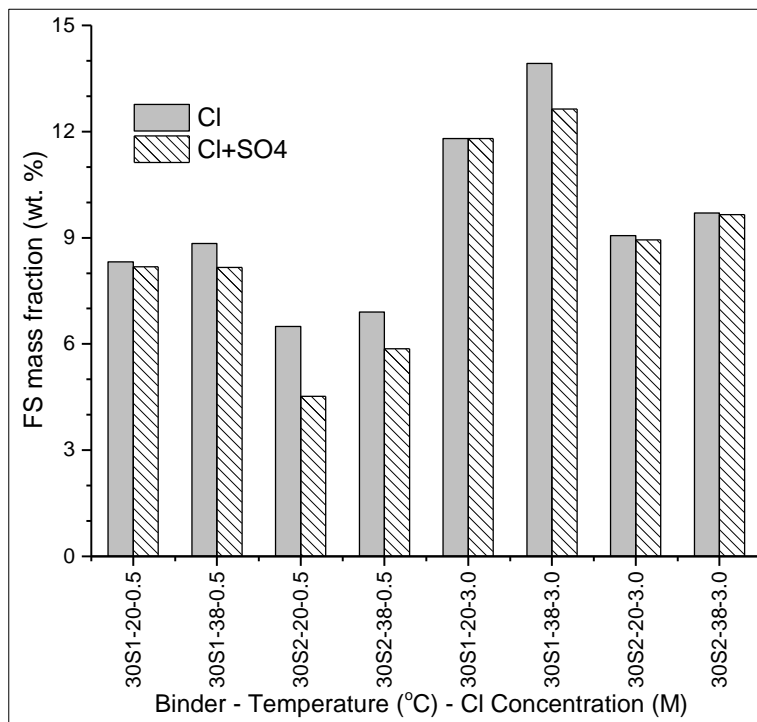
318

319 DTG peaks were more intense and FS decomposition occurred over a more narrow  
320 temperature range in the 30% slag samples than in the 70% slag samples. This is  
321 consistent with the XRD patterns and perhaps reflects a slightly less crystalline or  
322 ordered phase. There was no major difference in the decomposition temperature  
323 ranges for the pastes exposed to pure chloride solutions (Fig. 10).

324 TGA was used to quantify the Friedel's salt content in the various samples, to further  
325 highlight the effects of different factors including: temperature, slag composition, slag  
326 content, external sulphate and free chloride concentrations (Figs. 11 & 12). At 30%  
327 slag load (Fig.11), the presence of sulphate led to decreased presence of FS,  
328 consistent with chloride binding. This effect is more pronounced at 0.5M than 3.0M  
329 chloride concentration. At 70% slag content and 3.0M chloride concentration  
330 (Fig.12), the presence of sulphate did not impact on FS content. This is consistent  
331 with the XRD results (Fig.8b). There are two possible explanations for this. Firstly,  
332 the higher aluminate content ensures that there is no competition for aluminates

333 between sulphates and chlorides. Secondly, this supports previous findings that it is  
 334 the C-A-S-H phase in slag blended cements which accounts for the majority (~70%)  
 335 of total bound chloride in the paste [15]. This is also in line with Fig. 13 showing the  
 336 relationships between bound chloride and the formed FS for 30% and 70% slag  
 337 blends respectively. However, at 30% slag replacement and irrespective of chloride  
 338 concentration, a strong, statistically significant linear relationship was observed  
 339 between bound chloride and FS content, Pearson correlation = 0.803, p value =  
 340 0.000 (2-sided). Also, adjusted  $r^2 = 0.62$ . This was not the case for the 70% slag  
 341 blends and also shows a low adjusted  $r^2 = 0.16$ . As shown in Fig.13b for the 70%  
 342 slag blends, the relationship between bound chloride and FS at low chloride  
 343 concentration (0.5M) appears to be different from that at higher concentration (3.0M).  
 344 This finding indicates that FS formation is not the main precursor for chloride binding  
 345 at high slag replacement, supporting earlier finding in the literature [15].

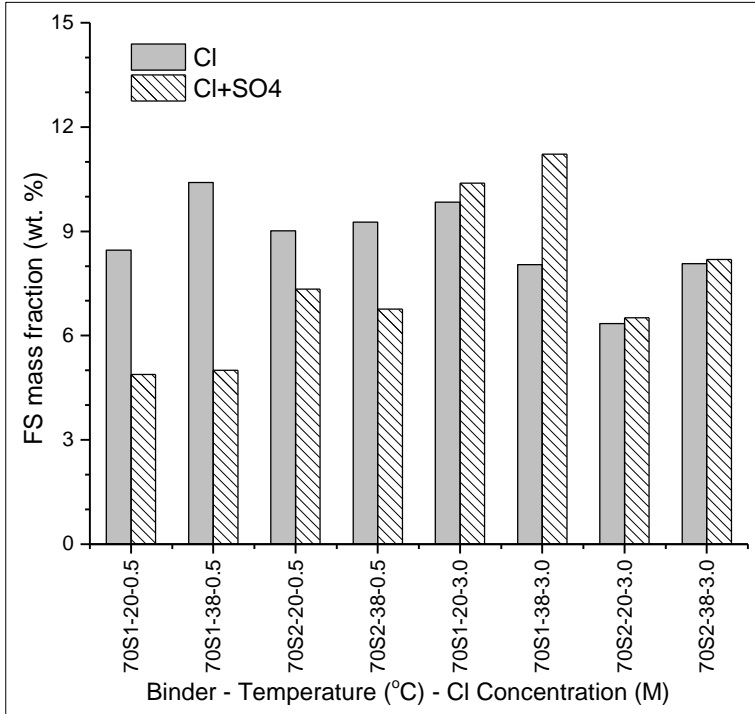
346



347

348 Fig. 11. Comparison between Friedel's salt contents determined by TGA for 30%  
 349 slag-blended pastes exposed to pure NaCl, and combined NaCl plus Na<sub>2</sub>SO<sub>4</sub>  
 350 solutions.

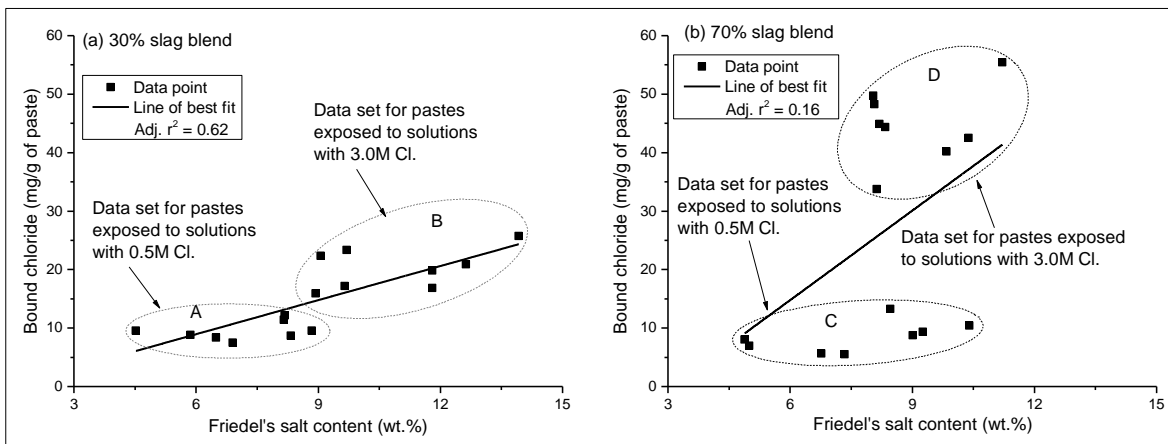
351



352

353 Fig. 12. Comparison between Friedel's salt contents determined by TGA for 70%  
 354 slag-blended pastes exposed to pure NaCl, and combined NaCl plus Na<sub>2</sub>SO<sub>4</sub>  
 355 solutions.

356



357

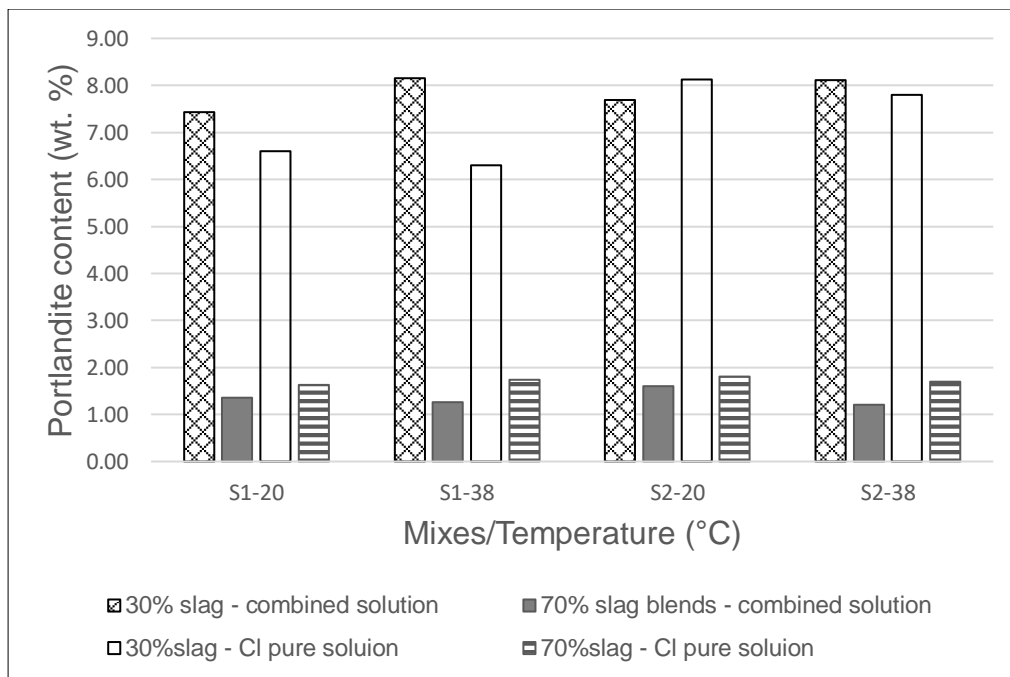
358 Fig. 13. Relationship between bound chloride and Friedel's salt (a) 30% slag blends,  
 359 (b) 70% slag blends

360

361 Fig. 14 shows portlandite contents determined by TGA following chloride binding in  
362 3.0M pure and combined chloride solutions. In all instances, portlandite contents  
363 were lower in the 70% blends than in the 30% blends. This is due to a combination  
364 of clinker dilution and the pozzolanic behaviour of the slag consuming the portlandite  
365 produced upon clinker hydration.

366 At 30% replacement, in most instances the CH content post-exposure was generally  
367 higher in the samples exposed to the combined solution than exposed to the pure  
368 chloride solution. This may be explained by the consumption of calcium from CH to  
369 stabilise FS, of which there was more present following exposure to the pure chloride  
370 solution. However, at 70% slag content this trend was reversed and also runs  
371 counter to the trends in FS contents as shown in Figures 11 and 12. This can be  
372 explained by the chloride binding relationships discussed earlier. Furthermore, the  
373 preferential reaction of sulphate with the aluminate-rich slag blend would require  
374 more calcium uptake to form monosulphate. As discussed earlier, depending on the  
375 concentration of the available chloride, sulphate is displaced to form KS at low  
376 chloride concentration or FS at high chloride concentration [49]. This agrees with the  
377 change in trend observed in Fig.12.

378



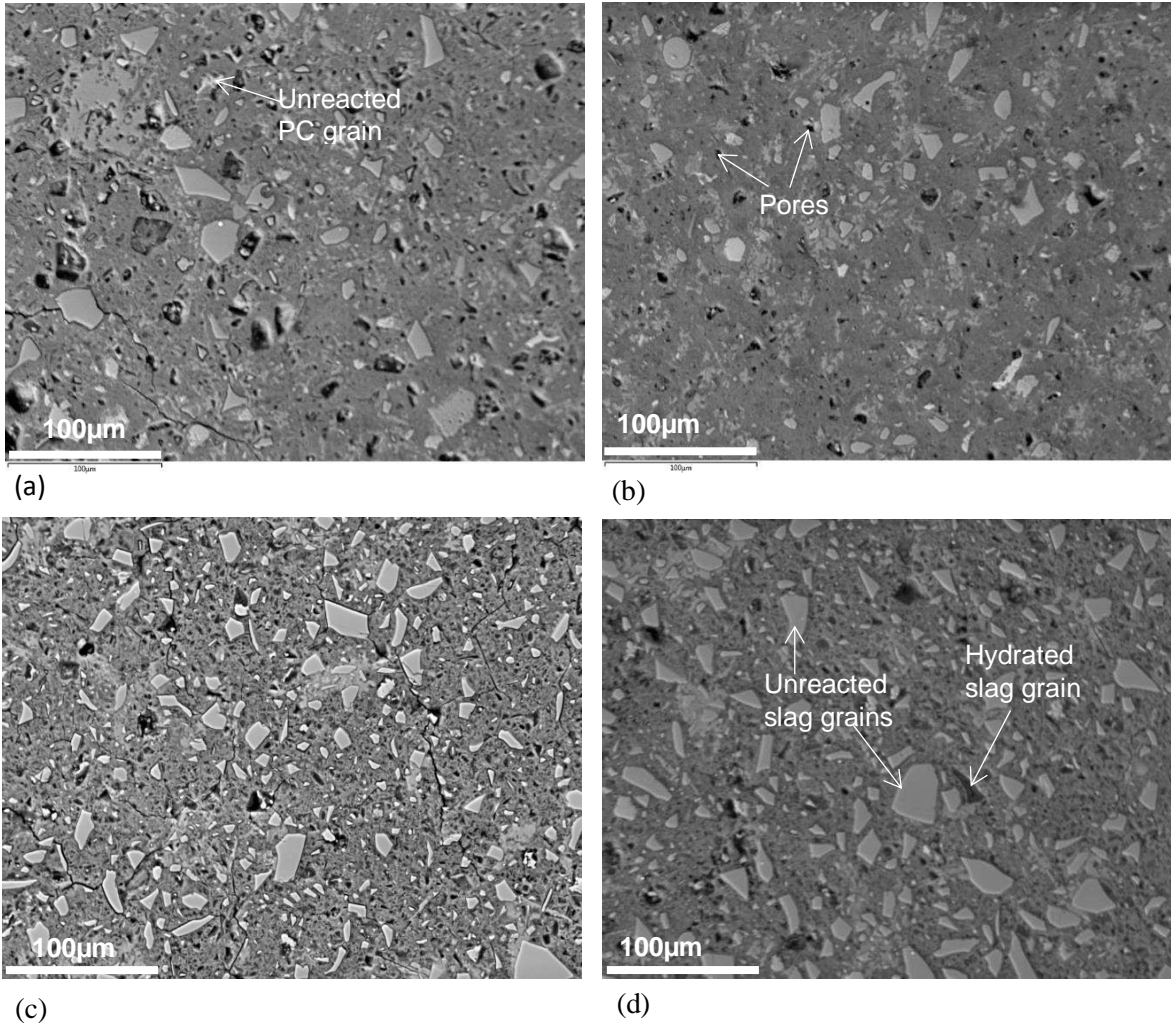
379

380 Fig. 14. Portlandite contents determined by TGA for pastes exposed to pure NaCl,  
 381 and combined NaCl plus Na<sub>2</sub>SO<sub>4</sub> solutions (Cl = 3.0M).

382

383 3.4 Degree of slag hydration from SEM/EDX-IA

384 Typical SEM-BSE micrographs for slag 1 blends at 20°C and 38°C are shown in Fig.  
 385 15, while Table 5 shows the degrees of clinker and slag hydration. Although, the  
 386 chloride binding paste samples were exposed to salt solutions after 56 days curing, it  
 387 was assumed that there would not be a considerable difference in the degrees of  
 388 hydration of the slag blends at 28 and 56 days. Hence, 28 days degrees of hydration  
 389 adopted here provides reasonable approximation of the later age hydration  
 390 characteristics of the pastes used for chloride binding investigation. Table 5 shows  
 391 that hydration of the slag blends increased slightly with increased temperature.  
 392 Meanwhile, there was a slight decrease in the degree of slag hydration with  
 393 increasing replacement, consistent with earlier findings [37]. However, the most  
 394 significant difference in the overall degree of hydration arose from changes in slag  
 395 content.



396

397 Fig. 15. SEM-BSE micrographs of slag blends hydrated for 28 days: (a) 30S1-20°C,  
 398 (b) 30S1-38°C, (c) 70S1-20°C, (d) 70S1-38°C.

399

400 Table 5. Degree of hydration from SEM-BSE image analysis

Age (day)	Mix	Wt.% of slag	Degree of hydration (%) at 20°C				Degree of hydration (%) at 38°C			
			Slag	Clinker	Weighted	Error	Slag	Clinker	Weighted	Error
28	30S1	30	63.22	94.53	85.137	0.60	67.57	96.02	87.485	0.52
	30S2	30	52.09	94.26	81.609	0.76	53.47	95.93	83.192	0.49
	70S1	70	62.11	98.47	73.018	0.77	63.32	99.84	74.276	0.60
	70S2	70	49.35	98.43	64.074	0.56	51.67	98.64	65.761	0.74

401

402 The increased chloride binding of the pastes with higher slag contents, despite  
 403 reduced degree of hydration, confirms the valuable contribution of slags to chloride  
 404 binding [43]. The aluminates in the unreacted slag grains may react with the  
 405 chlorides to contribute to increased chloride binding [34]. The results also show that

406 the alumina-rich slag 1 is more reactive, corresponding with the chloride binding  
407 results discussed earlier. Slag composition has a greater impact on the degree of  
408 slag hydration than does temperature, although, the situation is likely different at  
409 early age. This behaviour is consistent with findings about similar slag systems  
410 studied previously, where it was reported that increased hydration due to elevated  
411 temperatures reduced from between 11% and 14% at 7days, to between 5% and 8%  
412 at 28 days for 30% slag blends [29].

#### 413 **4. Conclusions**

414 This study has shown that chloride binding in slag-blended cements is affected by  
415 temperature and slag composition. However, the effects are different in pure chloride  
416 solutions and combined chloride-sulphate solutions. This is possibly because of the  
417 role of CH in stabilising the formation of FS. Chloride binding was slightly reduced in  
418 the presence of sulphate. Despite reduced degree of hydration, higher slag loading  
419 showed improved chloride binding, irrespective of whether the attacking solution was  
420 pure chloride, or combined chloride and sulphate. Friedel's salt formation correlated  
421 well with chloride binding at 30 wt% slag content. This was not the same for 70 wt%  
422 slag blends. This is attributed to the activity of alumina in the unreacted slag which  
423 may react with chloride to improve the chloride binding capacity of the pastes with  
424 higher slag contents, in addition to the reported high binding capacity of the C-A-S-H  
425 phase. Increase in temperature from 20°C to 38°C led to improved chloride binding,  
426 while blends containing a more basic, alumina-rich slag also bound more chlorides  
427 than a less basic slag with a lower alumina content. The trend in chloride binding  
428 concerning the influences of slag composition and temperature, were generally  
429 consistent with the slags degrees of hydration. Ettringite was displaced in the

430 combined solution at higher chloride concentration (3.0M) forming Friedel's salt,  
431 while Kuzel's salt was formed at lower concentration (0.5M).

432 The novelty of the study is the differentiation of chloride binding characteristics  
433 between low slag blends and high slag blends exposed to combined chloride-  
434 sulphate solutions, highlighting the effects of temperature and slag compositions.

435

### 436 **Acknowledgments**

437 The Niger Delta Development Commission (NDDC), Nigeria provided the PhD  
438 scholarship for this research. The facilities for carrying out the investigations were  
439 provided by the School of Civil Engineering at University of Leeds, UK.

440

### 441 **References**

- 442 [1] Yuan Q, Shi C, De Schutter G, Audenaert K, Deng D. Chloride binding of cement-based materials  
443 subjected to external chloride environment – A review. *Constr Build Mater.* 2009;23(1):1-13.
- 444 [2] Loser R, Lothenbach B, Leemann A, Tuchschnid M. Chloride resistance of concrete and its  
445 binding capacity – Comparison between experimental results and thermodynamic modeling.  
446 *Cement & Concrete Composites* 2010;32(2010):34-42.
- 447 [3] Arya C, Xu Y. Effect of cement type on chloride binding and corrosion of steel in concrete. *Cem*  
448 *Concr Res.* 1995;25(4):893 - 902.
- 449 [4] Ogirigbo OR, Black L. Chloride binding and diffusion in slag blends: Influence of slag composition  
450 and temperature. *Constr Build Mater.* 2017;149:816-25.
- 451 [5] Otieno M, Beushausen H, Alexander M. Effect of chemical composition of slag on chloride  
452 penetration resistance of concrete. *Cement & Concrete Research.* 2014;46:56-64.
- 453 [6] Backus J, McPolin D, Basheer M, Long A, Holmes N. Exposure of mortars to cyclic chloride  
454 ingress and carbonation. *Adv Cem Res.* 2013;25(1):3-11.
- 455 [7] Garcia V, François R, Carcasses M, Gegout P. Potential measurement to determine the chloride  
456 threshold concentration that initiates corrosion of reinforcing steel bar in slag concretes. *Mater*  
457 *Struct.* 2014;47(9):1483-99.
- 458 [8] Meira GR, Andrade C, Vilar EO, Nery KD. Analysis of chloride threshold from laboratory and field  
459 experiments in marine atmosphere zone. *Constr Build Mater.* 2014;55(Supplement C):289-98.
- 460 [9] Luo R, Cai Y, Wang C, Huang X. Study of chloride binding and diffusion in GGBS concrete. *Cem*  
461 *Concr Res.* 2003;33(1):1-7.
- 462 [10] Thomas MDA, Hooton RD, Scott A, Zibara H. The effect of supplementary cementitious materials  
463 on chloride binding in hardened cement paste. *Cem Concr Res.* 2012;42(2012):1-7.
- 464 [11] Caijun S, Xiang H, Xiaogang W, Zemei W, Geert de S. Effects of Chloride Ion Binding on  
465 Microstructure of Cement Pastes. *J Mater Civ Eng.* 2017;29(1):1-7.

- 466 [12] De Weerd K, Justnes H. The effect of sea water on the phase assemblage of hydrated cement  
467 paste. *Cem Concr Compos.* 2015;55:215-22.
- 468 [13] De Weerd K, Justnes H, Geiker MR. Changes in the phase assemblage of concrete exposed to  
469 sea water. *Cem Concr Compos.* 2014;47:53-63.
- 470 [14] Florea MVA, Brouwers HJH. Chloride binding related to hydration products: Part I: Ordinary  
471 Portland Cement. *Cem Concr Res.* 2012;42(2):282-90.
- 472 [15] Florea MVA, Brouwers HJH. Modelling of chloride binding related to hydration products in slag-  
473 blended cements. *Constr Build Mater.* 2014;64:421-30.
- 474 [16] Shi Z, Geiker MR, De Weerd K, Østnor TA, Lothenbach B, Winnefeld F, et al. Role of calcium on  
475 chloride binding in hydrated Portland cement–metakaolin–limestone blends. *Cem Concr Res.*  
476 2017;95:205-16.
- 477 [17] Galan I, Glasser FP. Chloride in cement. *Adv Cem Res.* 2015;27(2):63-97.
- 478 [18] Arya C, Buenfeld NR, Newman JB. Factors influencing chloride-binding in concrete. *Cem Concr*  
479 *Res.* 1990;20(2):291-300.
- 480 [19] De Weerd K, Orsáková D, Geiker MR. The impact of sulphate and magnesium on chloride  
481 binding in Portland cement paste. *Cem Concr Res.* 2014;65:30-40.
- 482 [20] Dehwah HAF. Effect of sulphate contamination on chloride binding capacity of plain and blended  
483 cements. *Adv Cem Res.* 2006;18(1):7-15.
- 484 [21] Geng J, Easterbrook D, Li LY, Mo LW. The stability of bound chlorides in cement paste with  
485 sulfate attack. *Cem Concr Res.* 2015;68:211-22.
- 486 [22] Maes M, De Belie N. Resistance of concrete and mortar against combined attack of chloride and  
487 sodium sulphate. *Cem Concr Compos.* 2014;53:59-72.
- 488 [23] Chen Y, Gao J, Tang L, Li X. Resistance of concrete against combined attack of chloride and  
489 sulfate under drying–wetting cycles. *Constr Build Mater.* 2016;106(Supplement C):650-8.
- 490 [24] Ukpata JO, Basheer PAM, Black L. Influence of temperature on the chloride binding of slag-  
491 blended cements in the presence of external sulphate. In: Bai Y, Zhang M, Shi S, editors. 37th  
492 Cement and Concrete Science Conference. London: The Institute of Materials, Minerals and  
493 Mining; 2017. p. 191-4.
- 494 [25] Zibara H. Binding of external chlorides by cement pastes [PhD]. Canada: University of Toronto;  
495 2001.
- 496 [26] Dousti A, Shekarchi M. Effect of exposure temperature on chloride-binding capacity of  
497 cementing materials. *Magazine of Concrete Research.* 2015;67(15):821 - 32.
- 498 [27] De Weerd K, Colombo A, Coppola L, Justnes H, Geiker MR. Impact of the associated cation on  
499 chloride binding of Portland cement paste. *Cem Concr Res.* 2015;68(Supplement C):196-202.
- 500 [28] Ogirigbo OR, Black L. The effect of slag composition and curing duration on the chloride ingress  
501 resistance of slag blended cements. *Adv Cem Res.* 2018;Published online: February 15,  
502 2018(0):1-34.
- 503 [29] Ogirigbo OR, Black L. Influence of slag composition and temperature on the hydration and  
504 microstructure of slag blended cements. *Constr Build Mater.* 2016;126:496-507.
- 505 [30] Ukpata JO, Basheer PAM, Black L. Performance of plain and slag-blended cements and mortars  
506 exposed to combined chloride–sulfate solution. *Adv Cem Res.* 2018;Published online: October,  
507 2017(0):1-16.
- 508 [31] BS EN 15167-1. Ground granulated blast furnace slag for use in concrete, mortar and grout. *Part*  
509 *1: Definitions, specifications and conformity criteria.*: BSI; 2006.
- 510 [32] BS EN 197-1. Cements Part 1: Composition, specifications and conformity criteria for common  
511 cements. Part 1: Composition, specifications and conformity criteria for common cements: BSI;  
512 2011.
- 513 [33] Tang L, Nilsson L-O. Chloride binding capacity and binding isotherms of OPC pastes and mortars.  
514 *Cem Concr Res.* 1993;23:247-53.
- 515 [34] Delagrave A, Marchand J, Ollivier J-P, Julien S, Hazrati K. Chloride Binding Capacity of Various  
516 Hydrated Cement Paste Systems. *Adv Cem Based Mater.* 1997;6:28-35.

- 517 [35] Ramachandran VS. Concrete Science. In: Ramachandran VS, Beaudoin JJ, editors. HANDBOOK OF  
518 ANALYTICAL TECHNIQUES IN CONCRETE SCIENCE AND TECHNOLOGY Principles, Techniques, and  
519 Applications. USA: WILLIAM ANDREW PUBLISHING; 2001. p. 1-55.
- 520 [36] Whittaker M, Zajac M, Ben Haha M, Black L. The impact of alumina availability on sulfate  
521 resistance of slag composite cements. *Constr Build Mater*. 2016;119:356-69.
- 522 [37] Whittaker MJ. The Impact of Slag Composition on the Microstructure of Composite Slag  
523 Cements Exposed to Sulfate Attack. Leeds: University of Leeds; 2014.
- 524 [38] Kocaba V, Galluci E, Scrivener KL. Methods for the determination of degree of reaction of slag in  
525 blended cement pastes. *Cement & Concrete Research*. 2012;42:511-25.
- 526 [39] Ogrigbo OR. Influence of Slag Composition and Temperature on the Hydration and Performance  
527 of Slag Blends in Chloride Environments: The University of Leeds; 2016.
- 528 [40] Maes M. Combined Effects of Chlorides and Sulphates on Cracked and Self-Healing Concrete in  
529 Marine Environments [PhD]. Ghent: Ghent University, Belgium; 2015.
- 530 [41] Frias M, Goñi S, García R, Villa RVdL. Seawater effect on durability of ternary cements. Synergy  
531 of chloride and sulphate ions. *Composites Part B, Engineering* 2013;46:173-8.
- 532 [42] Shaheen F, Pradhan B. Influence of sulfate ion and associated cation type on steel  
533 reinforcement corrosion in concrete powder aqueous solution in the presence of chloride ions.  
534 *Cem Concr Res*. 2017;91:73-86.
- 535 [43] Dhir RK, El-Mohr MAK, Dyer TD. Chloride binding in GGBS concrete. *Cem Concr Res*.  
536 1996;26(12):1767-73.
- 537 [44] Holden WR, Page CL, Short NR. The influence of chlorides and sulphates on durability. In: Crane  
538 AP, editor. *Corrosion of reinforcement in concrete*. London: Ellis Horwood Limited; 1983. p.  
539 143-50.
- 540 [45] Aldea C-M, Young F, Wang K, Shah SP. Effects of curing conditions on properties of concrete  
541 using slag replacement. *Cem Concr Res*. 2000;30(3):465-72.
- 542 [46] Humam T, Siddique R. Properties of Mortar Incorporating Iron Slag. *Leonardo Journal of*  
543 *Sciences*. 2013;1(23):53-60.
- 544 [47] Ipavec A, Vuk T, Gabrovšek R, Kaučič V. Chloride binding into hydrated blended cements: The  
545 influence of limestone and alkalinity. *Cem Concr Res*. 2013;48(Supplement C):74-85.
- 546 [48] Mesbah A, François M, Cau-dit-Coumes C, Frizon F, Filinchuk Y, Leroux F, et al. Crystal structure  
547 of Kuzel's salt  $3\text{CaO}\cdot\text{Al}_2\text{O}_3\cdot\frac{1}{2}\text{CaSO}_4\cdot\frac{1}{2}\text{CaCl}_2\cdot 11\text{H}_2\text{O}$  determined by synchrotron powder  
548 diffraction. *Cem Concr Res*. 2011;41(5):504-9.
- 549 [49] Balonis M, Lothenbach B, Le Saout G, Glasser FP. Impact of chloride on the mineralogy of  
550 hydrated Portland cement systems. *Cem Concr Res*. 2010;40(7):1009-22.
- 551 [50] Birnin-Yauri UA, Glasser FP. Friedel's salt,  $\text{Ca}_2\text{Al}(\text{OH})_6(\text{Cl},\text{OH})\cdot 2\text{H}_2\text{O}$ : its solid solutions and their  
552 role in chloride binding. *Cem Concr Res*. 1998;28(12):1713-23.
- 553 [51] Grishchenko RO, Emelina AL, Makarov PY. Thermodynamic properties and thermal behavior of  
554 Friedel's salt. *Thermochim Acta*. 2013;570:74-9.
- 555 [52] Shi Z, Geiker MR, Lothenbach B, De Weerd K, Garzón SF, Enemark-Rasmussen K, et al. Friedel's  
556 salt profiles from thermogravimetric analysis and thermodynamic modelling of Portland  
557 cement-based mortars exposed to sodium chloride solution. *Cem Concr Compos*. 2017;78:73-  
558 83.